Synthesis and characterization of DTPA and DOTA modified Fe$_3$O$_4$@SiO$_2$ core-shell nanoparticles

Elham Sattarzadeh Khameneh [1], Saeed Kakaei *,[1], Mohammad Moein Moharreri [2]

[1] Materials and Nuclear Fuel Research School, Nuclear Science and Technology Research Institute, Tehran, Iran
[2] Department of Polymer, Faculty of Technical and Engineerin, Golestan University, P. O. Box 155, Gorgan, Golestan, Iran

Abstract

Chelation is a type of ions/ molecules bonding to metal ions. Due to the excellent chelating properties of aminopolycarboxylic acids such as diethylenetriaminepentaacetic acid (DTPA) and 1,4,7,10-tetraazacyclododecane-1,4,7,10-tetraacetic acid (DOTA), this study focuses on the synthesis of these compounds. Few investigations have been carried out on the comparison of desorption rate and amount of heavy metals extracted successively by organic acid mixtures. DTPA and DOTA as chelating agents were grafted on the metal nanoparticles (MNPs). They are convenient compounds for the removal of heavy metals ions from wastewater. Magnetic iron oxide nanoparticles with narrow size distribution were synthesized by a simple and high-yielded co-precipitation technique using ferrous salts with molar ratio of Fe^{3+}/Fe^{2+}=2. After preparation of silica-coated iron oxide nanoparticles by Stöber method (wet chemistry), the nanoparticles were functionalized via amine residues of ligands. The synthesis of Fe$_3$O$_4$@SiO$_2$ core-shell nanoparticles, as well as their structural and magnetic properties, were characterized by X-ray diffraction (XRD), tramsition electron microscopy (TEM), Fourier-transform infrared (FT-IR) spectroscopy, Brunauer-Emmett-Teller (BET), and thermogravimetric analysis techniques.
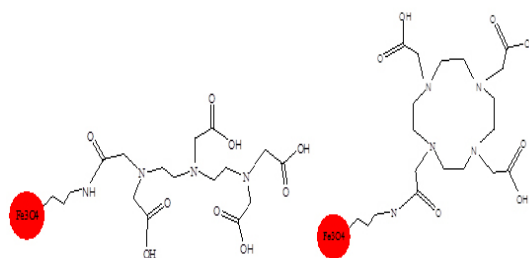
Keywords: *Fe$_3$O$_4$@SiO$_2$ core–shell nanoparticles, DTPA, DOTA, Surface functionalization.*

Introduction

Heavy metals are one of the most dangerous environmental contaminants that have a relatively high density compared to water. The contamination of water and soil recourses by heavy metal is a serious worldwide problem. These elements enter into the soil and water, and it is very difficult to eliminate their effects.[1] Industrial activities, mining and coal combustion are typical examples of heavy metal contaminations.[2] The removal of these metals is crucial because of their non-biodegradability and toxicity which often accumulate in the food chain.[3,4] Extensive research has been carried out to introduce materials which can remove and alleviate heavy metals.[2] Chemical precipitation, ion exchange, and adsorption are three commonly used methods for heavy metals elimination. Among them, adsorption has attracted many attentions since new material types are available for the removal process according to their application. Some of these materials are zeolites, activated carbon, fly ash, resins, chelating agent, and so on.[2,5]

At high concentrations (higher than 100 mg/L), elimination is achieved by a chemical precipitation method but at lower concentrations, the removal of heavy metal is better achieved by adsorption. One of the most interesting materials that can be used as adsorbent is chelating agents such as diethylenetriaminepentaacetic acid (DTPA), 1,4,7,10-tetraazacyclododecane-1,4,7,10-tetraacetic acid (DOTA), ethylenediaminetetraacetic acid (EDTA), etc.

They can be stable in a solid or liquid state characterized by two valences, auxiliary and principal. Chelating agents are typically characterized by a functional group containing donor atoms such as O, N, S, and P which can coordinate to different metal ions. Coordination number is the number of ligand atoms that bound to the metal. The primary valency also called the oxidation state (1$^+$, 2$^+$, 3$^+$), typically has coordination numbers of 4 or 6, with less common values of 2, 3, 5, 7, 8, 9 and even 10. Chelating agents are expected to have the ability to form stable complexes with metals and reverse the metal binding after being treated chemically.[4,6]

DTPA has a high affinity for metal cations. Thus, the DTPA^{5-} anion is potentially an octadentate ligand assuming that each nitrogen and COO$^-$ group counts as a center for coordination. The formation constants for its complexes are about 100 time greater than those for EDTA. As a chelating agent, DTPA envelopes around a metal ion by forming up to eight bonds. DTPA is effective for Co (II), Cd (II), Cu (II), Zn (II), and Ni (II) removal from contamination. In the previous studies, adsorption of metals such as Cd(II), Pb(II), Co(II), and Ni(II) by DTPA adsorbents has quite extensively studied.[7-9] DOTA wraps metal cations but the geometry of the ligand depends on the geometric tendencies of the metal cation. The main applications involve the lanthanides (such as Nd^{3+}, Eu^{3+}, Tm, Ho^{3+}, Dy^{3+}, Lu^{3+}, and Sr^{2+}) and in such complexes DOTA functions as an octadentate ligand binding the metal through four amine and four carboxylate groups. For most transition metals (such as Cu^{2+}, Ni^{2+}, Co^{2+}, Zn^{2+}, and Fe^{3+}), DOTA functions as a hexadentate ligand binding through the four nitrogen and two carboxylate centers. The

Corresponding author:
Saeed Kakaei, Email: Skakaei@aeoi.org.ir

complexes have octahedral coordination geometry with two pendent carboxylate groups.[10-13]

In this study, the materials that could be used as good adsorbent were introduced. These complexes contain magnetic iron oxide core-shell nanoparticles (NPs) that are coupled to the molecules such as DTPA and DOTA as chelating agents.[14] Separation is one of the problems in the use of a chelating agent as an adsorbent. However, the application of magnetic NPs provides the possibility to easily collect and isolate the adsorbent materials after the adsorption of metals into these complexes by an external magnet.

Given the immense importance of magnetic NPs, there has been a widespread interest in accessing the above adsorbent. In this respect, the preparation of core-shell nanostructure was recently reported by the current researchers in which its potential in therapeutic and diagnostic applications was evaluated.[14-16,19]

In the present study, an attempt was made to synthesize magnetic NPs and then chelating agents (DTPA and DOTA) which were coupled to the NPs as adsorbent. The core-shell structures were characterized by X-ray diffraction (XRD), transmission electron microscopy (TEM), Fourier-transform infrared (FT-IR) spectroscopy, Brunauer-Emmett-Teller (BET), and thermogravimetric analysis techniques. These complexes have the potential to be used as an adsorbent for the removal of heavy metals.

Experimental

Materials and methods

Tetraethoxysilane (TEOS, 99%, Fluka), (3-Aminopropyl) triethoxysilane (APTES, 99%, Aldrich), iron(III) chloride hexahydrates ($FeCl_3.6H_2O$, 98%, Fluka), iron(II) chloride tetrahydrates ($FeCl_2.4H_2O$, 99%, Fluka), 1,4,7,10-tetraazacyclododecane-1,4,7,10-tetraacetic acid mono(N-hydroxysuccinimide ester) (DOTA-NHS, 99%, Merck), toluene (99%, Merck), absolute ethanol (EtOH, 99%, Merck), ammonia (NH_3 25%, Merck) were purchased and used without any further purification. Infrared spectra were recorded on Bruker VECTOR 22 FT-IR spectrometer. X-ray diffraction patterns of samples were obtained using powder XRD, a Phillips PW-1800 diffractometer with Cu-K_α radiation (λ= 1.5402 Å). Thermogravimetric/ differential thermal analyzer (TG/DTA) was performed by TG/DTA instrument model 6300 and the results were used to determine organic content in samples.

Synthesis of the DTPA and DOTA-modified $Fe_3O_4@SiO_2$ core-shell structures

Fe_3O_4 NPs were prepared by co-precipitation of ferric chloride ($FeCl_3.6H_2O$) and ferrous chloride ($FeCl_2.4H_2O$) in a molar ratio of 1:2 in distilled water at 80 ℃ under nitrogen gas protection. After adding ammonium hydroxide, the mixture was stirred for 25 min. Next, the black product was collected by a magnet and washed three times with distilled water, followed by washing with ethanol once.[14,15] The Stöber method was used for the preparation of core-shell structure ($Fe_3O_4@SiO_2$). Fe_3O_4 NPs were dispersed in a mixture of ethanol/water (4:1, v/v). The pH of the solution was adjusted to 9 by adding ammonia and TEOS was added. The solution was stirred at 40℃ for 12 h. The precipitate was collected and washed with water.[16] Silica-coated magnetite NPs were added to a freshly prepared solution of APTES in water (2% v/v) and the mixture was stirred at room temperature for 24 h.[17] Finally, amine functionalized magnetic NPs ($Fe_3O_4@SiO_2$-APTES) were separated by a magnet and washed copiously with toluene. The dry DTPA was activated with DDC and NHS (in NaOH solution, pH=6, 2 h in dark).

The colloidal solution of APTES-modified NPs was added and stirred in the dark at room temperature for 12 h. Moreover, another chelating agent (DOTA) was added to the NPs (pH= 8.5, 12 h, room temperature). Finally, the products (core shell-DTPA and core shell-DOTA) were collected by a magnet and washed several times with distilled water.[14,18]

Results and discussion

FT-IR spectroscopy

To confirm the coating of the magnetite surface through the silanization reaction, an FT-IR spectrum of the APTES-SiO_2-magnetite was obtained (Figure 1). The main absorption bands of OH (3470 cm^{-1}) and Fe-O-Fe (590 cm^{-1}) groups were observed. The adsorption of silane polymer on the magnetite particles surface was confirmed by bands at 1034 and 1125 cm^{-1} assigned to the SiO–H and Si–O–Si groups. The two broad bands at 3470 and 1632 cm^{-1} can be ascribed to the N–H stretching vibration and NH$_2$ bending mode of free NH$_2$ group, respectively.[19,20]
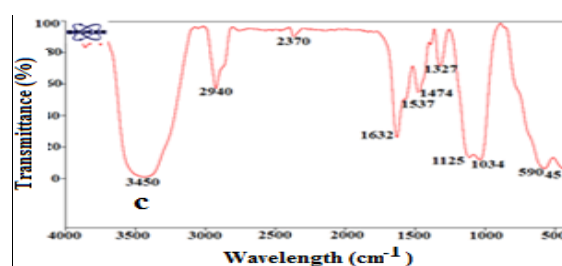

Figure 1. The FT-IR spectra of APTES-SiO$_2$-magnetite.

To confirm the bonding of the magnetite surface with DTPA and DOTA, FT-IR spectra were obtained (Figure 2a and 2b). The bands in the 2800-2900 cm^{-1} region which were intensified in comparison to that of the IR spectrum of APTS-$SiO_2@Fe_3O_4$ can be ascribed to the C–H stretching vibration of DTPA and DOTA together with C–H starching vibration bands of APTS. The two broad bands at 1628 and 1574 cm^{-1} can be ascribed to the C=O stretching vibration. The absorption bands of C-O (1307 cm^{-1}), and C-N (1061 cm^{-1}) groups were observed. These bands demonstrated chelating agents were coupled successfully on the surface of APTS-$SiO_2@Fe_3O_4$.
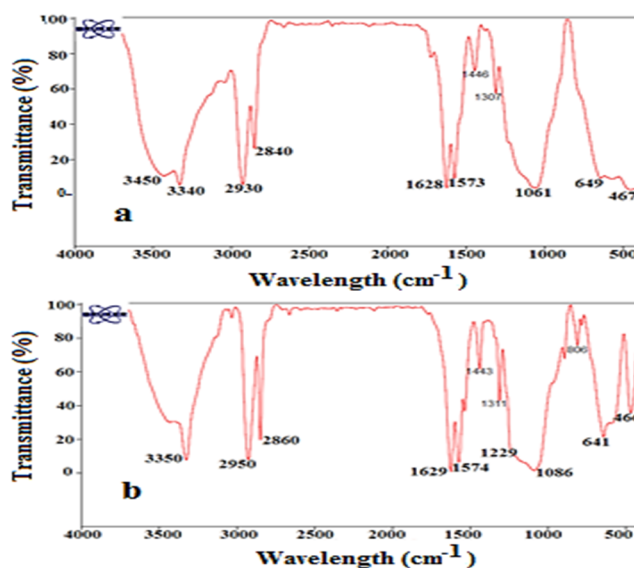

Figure 2. The FT-IR Spectra of (a) core shell-DTPA and (b) core shell-DOTA.

X-ray powder diffraction

The X-ray diffraction (XRD) patterns showed that the standard Fe_3O_4 crystal with spinel structure has six diffraction peaks with $2\theta=$ 22, 31.1, 40, 42.2, 51.1, and 44.0°. On the other hand, no peaks were detected in silica-coated Fe_3O_4 NPs which could be assigned to impurities as shown in Figure 3b and the broad diffraction in the range of 16-25° is due to the amorphous silica shell that was coated on the surface of iron oxide in reaction with TEOS. The diffraction patterns of magnetite Fe_3O_4 and APTS-SiO_2@Fe_3O_4 were in accordance with the XRD pattern of pure Fe_3O_4 phase (cubic phase, JCPDS card 19-0629). This displayed that the Fe_3O_4 NPs remained unchanged during functionalization.[21] An average particles size nanoparticles using Scherrer equation ($D = k\lambda/(\beta \cos\theta)$).
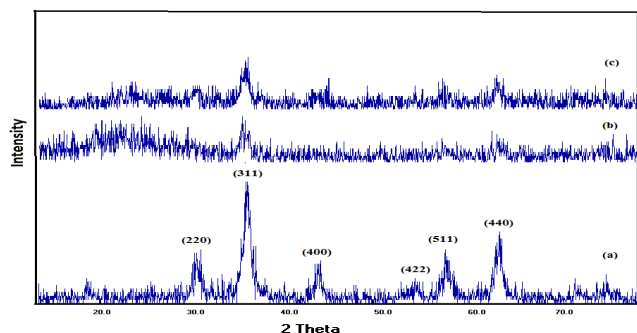
Figure 3. The XRD patterns of (a) Fe_3O_4, (b) Fe_3O_4@SiO_2, and (c) $Fe_3O_4SiO_2$-APTES.

Thermogravimetric analysis

Thermogravimetric analysis (TG) was carried out to determine the characterization of the organic components over the surface of Fe_3O_4. In all curves, the first mass loss, below 150°C is related to the adsorbed water and residual ethanol, while the second mass loss within the temperature range from 250 to 700°C can be ascribed to the thermal decomposition of organic contents such as 3-aminopropyl, DTPA, and DOTA groups.[22,23]
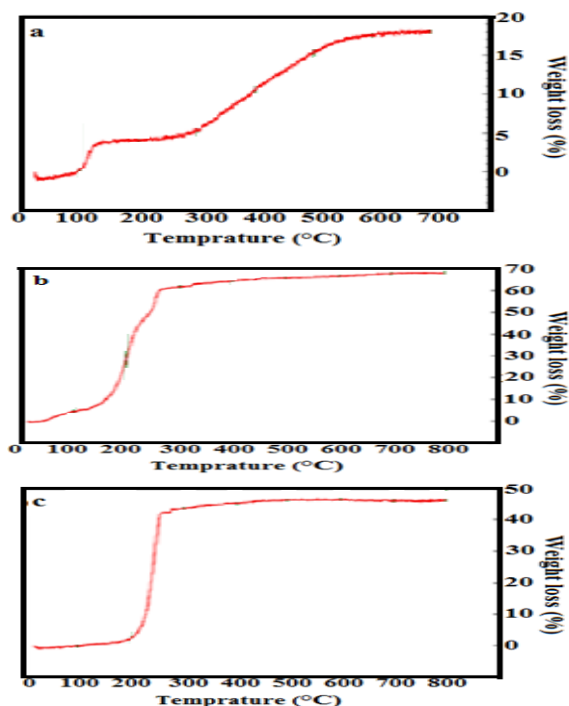
Figure 4. The thermograms of (a) APTS-SiO_2@Fe_3O_4, (b) DTPA/APTS-SiO_2@Fe_3O_4, and (c) DOTA/APTS-SiO_2@Fe_3O_4.

The TGA curve of APTS-SiO_2@Fe_3O_4 exhibits two steps of mass loss (Figure 4a). The first mass loss, about 4%, below 150°C is associated with the evaporation of adsorbed water and the second mass loss within the temperature range from 250 to 600°C can be attributed to the thermal decomposition of 3-aminopropyl groups. The thermogram of DTPA/APTS-SiO_2@Fe_3O_4 (Figure 4b) also presents two steps. Interestingly, below 150°C, the mass loss rate is slow, because losing the residual water adhering to the sample surface and adsorbing in the DTPA cavities. The second event with 64 % mass loss within the temperature range from 150 to 600°C is associated with the decomposition and breakdown of DTPA and organic residue. According to the thermogram of DOTA/APTS-SiO_2@Fe_3O_4 (Figure 4c), the second mass loss is about 42% of total mass loss.

TEM image

The morphology of magnetic NPs before and after functionalizing with APTES was studied by transmission electron microscopy (TEM) (Figure 5). The TEM observations indicate that the core-shell structure is spherical with narrow size distribution and successfully coated with APTES. The average size of Fe_3O_4@SiO_2, and Fe_3O_4@SiO_2–APTES is less than 10 nm and 20 nm, respectively that have good conformity with XRD result.
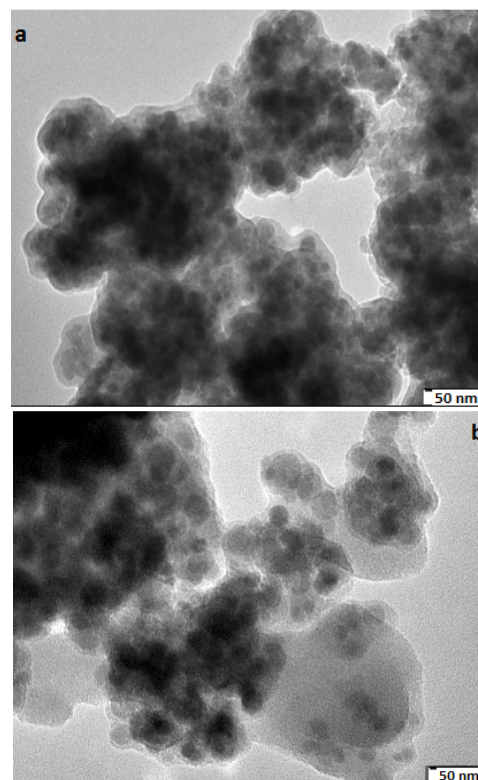
Figure 5. The TEM image of the (a) Fe_3O_4@SiO_2 and (b) Fe_3O_4@SiO_2–APTES nanostructures.

Conclusion

Superparamagnetic Fe_3O_4 nanocrystals of 6–7 nm diameters were synthesized by a chemical co-precipitation method, and a silica layer of about 2 nm thickness was coated on the nanocrystal surface by hydrolysis of TEOS (according to the TEM images and results of X-ray diffraction). The thickness of the silica layer can be easily adjusted by changing the ratio of TEOS to Fe_3O_4. The amino (–NH_2) groups were successfully covalently bonded to the coated

Fe_3O_4 nanocrystals and then DTPA and DOTA molecules were grafted on the nanocrystal surface through the reaction of $-NH_2$ and $-COOH$ as characterized by FT-IR spectra and TG analysis. According to the XRD observations, the present magnetic nanocrystals have a cubic spinel structure. This structure can be used for the removal and elimination of heavy metals owing to the existence of chelating agents as adsorbent. Further research is needed to investigate the absorption of metals using these core-shell structures.

Acknowledgments

References

1. G. Mulbachova, *Rost. Vyroba*, 48, **2002**, 536.
2. A. Baraka, P. J. Hall, M. J. Heslop, *React. Funct. Polym.*, 67, **2007**, 585.
3. T. G. Kazi, N. Jalbani, N. Kazi, *Biol. Trace Elem. Res.*, 125, **2009**, 16.
4. E. Repo, T. A. Kurniawan, J. Warchol, M. E. T. Sillanpää, *J. Hazard Mater.*, 171, **2009**, 1071.
5. P. K. Roy, A. S. Rawat, P. K. Rai, Talenta, 59, **2003**, 239.
6. G. Crini, *Prog. Polym. Sci.*, 30, 2005, 38.
7. E. Repo, J. K. Warchol, T. A. Kurniawan, M. E. T. Sillanpa, *Chem. Eng. J*, 161, **2010**, 73.
8. F. Zhao, E. Repo, M. Sillanpää,Y. Meng, D. Yin, W. Z. Tang, *Ind. Eng. Chem. Res*, 54, **2015**, 1271.
9. Sh. Akhtar, Sh. Iram, *J. Sci. Eng. Res.*, 5, **2014**, 536.
10. V. Villegas, N. Doyle, P. Robert, *Coord. Chem. Rev.*, 253, **2009**, 1906.
11. V. Fomenko, T. N. Polynova, M. A. Porai-Koshits, G. L. Varlamova, N. I. Pechurova, *J. Struct. Chem.*, 14, **1973**, 529.
12. D. Mohan, P. Kunwar, Water Res., 36, **2002**, 2304.
13. Y. Sağ, Ü. Açikel, Z. Aksu, T. Kutsal, *Process Biochem.*, 33, **1998**, 273.
14. Z. Pourmanouchehri, M. Jafarzadeh, S. Kakaei, E. Sattarzadeh, *J. Inorg. Organomet. Polym. Mater.*, 28, **2018**, 1980.
15. Y. He, Q. Wang, C. R. Li, Y. M. Miao, Z. Y. Wu, B. S. Zou, *J. Phys. D.: Appl. Phys.*, 38, **2005**, 1342.
16. W. Stöber, A. Fink, E. Bohn, *J. Colloid Interface Sci.*, 26, **1986**, 62.
17. K. Kim, S. Kim, Y. Chao, H. T. Kim, *J. Ind. Eng. Chem.*, 13, **2007**, 1137.
18. A. Abdukayum, C. X. Yang, Q. Zhao, J. T. Chen, L. X. Dong, X.P. Yan, *Ana. Chem.*, 86, **2014**, 4096.
19. A. Rizzuti, M. Dassisti, P. Mastrorilli, M. C. Sportelli, N. Cioffi, R. A. Picca, E. Agostinelli, G. Varvaro, R. Caliandro, *J. Nanopart. Res.*, 17, **2015**, 408.
20. K. Do. Kim, S. S. Kim, Y. H. Choa, H. T. Kim, *J. Ind. Eng. Chem.*, 13, **2007**, 1137.
21. O. Rahman, S. Chandra, Sh. Ahmad, *Mater. Chem. Phy.*, 132, **2012**, 196.
22. E. Sattarzadeh, M. M. Amini, S. Kakaei, A. Khanchi, *Radiochim. Acta*, 106, **2018**, 897.
23. E. Sattarzadeh, M. M. Amini, S. Kakaei, A. Khanchi, *J. Radioanal. Nucl. Chem.*, 317, **2018**, 1333.